Stereochemistry of the Fe(II)− and Fe(III)−Cyanide Complexes of the Homodimeric *Scapharca inaequivalvis* Hemoglobin. A Resonance Raman and FTIR Study

Alberto Boffi* and Emilia Chiancone

CNR Center of Molecular Biology and Department of Biochemical Sciences, University La Sapienza, 00185 Rome, Italy

Satoshi Takahashi

Riken, Laboratory of Biophysical Chemistry, Hirosawa 2-1, Wako City, Saitama Prefecture, 351-01, Japan

Denis L. Rousseau

Department of Physiology and Biophysics, Albert Einstein College of Medicine, Bronx, New York 10461

Received July 30, 1996; Revised Manuscript Received December 5, 1996[⊗]

ABSTRACT: Resonance Raman measurements carried out in parallel on ferrous and ferric *Scapharca inaequivalvis* dimeric hemoglobin cyanide derivatives allowed the identification of the electron density marker bands and heme core size marker bands in both derivatives in comparison with those obtained for the carbonmonoxy and deoxy adducts. The iron cyanide stretching mode, measured for the first time in a ferrous hemoprotein, has been detected at 455 cm^{-1}, only 6 cm^{-1} lower than in the corresponding ferric derivative. This finding demonstrates that the large free energy difference for complex formation between the two derivatives is not concentrated on the Fe−C bond. The internal stretching frequencies of the ligand in the ferric and ferrous derivatives have been identified by FTIR and Raman measurements using different cyanide isotopes. The frequency decreases in the order Fe(III)−CN adduct, free cyanide, Fe(II)−CN adduct, consistent with the behavior observed in inorganic complexes and horseradish peroxidase. The main feature emerging from these data is that cyanide, at variance with oxygen and carbon monoxide, binds to ferrous iron with only a minor perturbation of the electronic structure of the heme. The functional counterpart of this effect is the absence of cooperative cyanide binding in HbI.

Cyanide has been widely used to probe the hemoprotein binding site in that it is one of the few ligands which can bind to both ferric and ferrous heme iron. Cyanide, like carbon monoxide, binds to the ferric heme iron in a linear fashion in unhindered heme model compounds (Peng & Ibers, 1976). A long iron−carbon interatomic distance (Conti et al., 1993; Nardini et al., 1995) and a low bond stretching frequency (Tanaka et al., 1984; Yu et al., 1984) have been reported in a number of proteins and heme model compounds in the ferric form, indicating that the high stability of these complexes is not determined by the iron−carbon bond strength. The distortion from the preferred linear coordination observed in all hemoproteins studied to date has been accounted for by the steric pressure exerted by protein residues in the distal pocket (Deatherage et al., 1976) and/or by strong hydrogen bond interactions with positively charged amino acid residues in the vicinity of the bound ligand (Conti et al., 1993). Very few observations have been reported on the ferrous hemoprotein cyanide complexes in view of their very low stability and high photosensitivity. Horseradish peroxidase (Rakshit & Spiro, 1974) and cytochrome *c* oxidase (Ching et al., 1985) are the only ferrous cyanide hemoproteins investigated by resonance Raman spectroscopy.

This study demonstrates that cyanide binds to the ferrous heme iron yielding a low-spin derivative. Current ideas on the stereochemistry of the ferrous heme iron cyanide complex are based on the analogy between the electronic structures of cyanide anion and carbon monoxide. FTIR measurements on horseradish peroxidase, horse myoglobin, microperoxidase, and heme model compounds have shown that the cyanide stretching frequency decreases upon binding to the ferrous heme iron, as observed also in the case of CO and O_2 (Yoshikawa et al., 1985; Reddy et al., 1996). Moreover, transient kinetic experiments indicated that cyanide dissociates from ferrous HbA in a cooperative fashion, which is reminiscent of the behavior of oxygen (Brunori et al., 1992). Hence, cyanide binding to the ferrous heme appears to mimic the behavior of other ligands and thus can provide useful information for the understanding of hemoprotein function. However, in the absence of structural data on any ferrous cyanide hemoprotein, a direct comparison between cyanide and other ligands cannot be carried out in terms of stereochemistry and/or energetics of the bond.

The homodimeric hemoglobin (HbI) is the minor component present in the red cells of the blood clam *Scapharca inaequivalvis*. It is characterized by a moderately low oxygen affinity ($p_{1/2}$ = 8 mmHg), high cooperativity (Hill coefficient of 1.5), and absence of allosteric effectors (Chiancone et al., 1983). In HbI the structural basis for cooperative ligand binding differs from that characteristic of tetrameric vertebrate hemoglobins as the two heme groups

* Corresponding author. Fax: 39 6 44 40 062.

[⊗] Abstract published in *Advance ACS Abstracts,* March 1, 1997.

S0006-2960(96)01888-0 CCC: $14.00

are not exposed to solvent but are almost in direct contact at the subunit interface. In HbI, therefore, information transfer between hemes is direct and is accompanied by major tertiary changes at the heme pocket, with only minor quaternary rearrangements (Royer et al., 1989). HbI offers a unique possibility for the measurement of the stereochemical properties of the heme iron cyanide grouping since it is the only hemoglobin which forms stable cyanide complexes in both its oxidized and reduced state (Boffi et al., 1996). In fact, ferrous HbI binds the cyanide anion with an affinity constant of 17 M^{-1}, a value which is about 10-fold higher than that reported for sperm whale myoglobin (Keilin & Hartree, 1955). At variance with HbA, cyanide binding in HbI is not cooperative. The affinity of ferric HbI for the cyanide anion is a factor of 10^7 higher than in the ferrous derivative. In HbI the main contribution to the stabilization of bound cyanide is provided by the low polarity of the heme pocket which favors formation of the bond between the negatively charged cyanide and the positively charged iron. In HbI, the two hemes are shielded from solvent since they are at the subunit interface (Royer et al., 1989) and, in view of the absence of charged amino acid residues in the vicinity of the heme, provide an apolar environment for ligand binding (Ilari et al., 1995). This specific aspect of the HbI heme pocket is reflected in a slow rate of cyanide release, which is about 0.01 s^{-1} in the ferrous complex and 6×10^{-6} s^{-1} in the ferric complex, whereas the association rate constant is very similar to those measured for other hemoglobins and myoglobins (Brancaccio et al., 1994). In this framework, the large differences in kinetic and thermodynamic behavior of the ferric vs ferrous cyanide complexes in HbI and in horse myoglobin have been ascribed, to a first approximation, to the difference in the bond energy between the two derivatives (Boffi et al., 1996; Reddy et al., 1996).

In the present paper a spectroscopic characterization of the iron cyanide grouping has been carried out by resonance Raman and FTIR techniques. In particular, the iron cyanide stretching frequency has been measured for the first time in a ferrous derivative, allowing a direct comparison with the ferric complex and with other ferrous derivatives in HbI. The stereochemistry of the ferrous cyanide complex has been correlated to the unique structural and functional properties of HbI.

MATERIALS AND METHODS

S. inaequivalvis HbI was extracted and purified as described previously (Chiancone et al., 1981). The ferric protein was obtained by addition of excess (50:1 molar ratio) potassium nitrite to the oxygenated protein. The excess oxidant and its byproducts were removed by gel filtration on a Sephadex G-25 column equilibrated with 0.1 M borate buffer at pH 9.2. A slight excess of KCN was then added to obtain the ferric cyanide derivative. Ferrous−CN HbI was prepared under a nitrogen box by adding to the deoxygenated protein solution an equal volume of 1 M KCN buffered with boric acid at pH 9.2 in the presence of 50 mM sodium dithionite.

Resonance Raman spectra were measured at a protein concentration of about 100 μM (heme). A krypton ion laser with outputs at 413 and 407 nm and a frequency-doubled Ti-sapphire tuned to 428.5 nm were used to excite the resonance Raman spectra. The scattered light was dispersed by a single polychromator with a 1200 groove/nm grating and detected by a cryogenically cooled CCD camera. The spectral slit width was 5 cm^{-1}. The Rayleigh scattering was removed from the scattered light with a holographic filter.

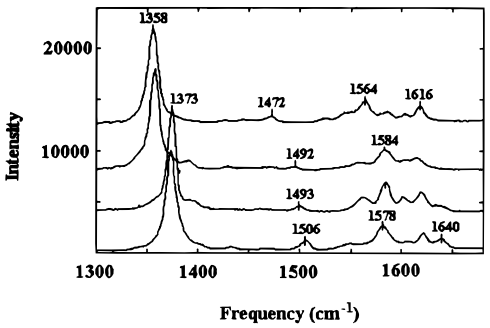

FIGURE 1: Resonance Raman spectra of HbI derivatives in borate buffer, pH 9.2. From top to bottom: deoxy, ferrous cyanide, carbonmonoxy, and ferric cyanide HbI. The buffer concentration was 0.1 M in all samples with the exception of ferrous cyanide HbI (1 M). Laser excitation wavelength: 407 nm for ferric cyanide HbI, 413 nm for carbonmonoxy HbI, and 428.5 nm for deoxy and ferrous cyanide HbI. The laser power was 40 mW for deoxy and ferric cyanide HbI and about 10 mW for ferrous cyanide and carbonmonoxy HbI.

FTIR measurements were carried out on a Matthson FTIR spectrometer with 4 cm^{-1} resolution, using a set of CaF_2 windows and a 500 μm teflon spacer. The sample was concentrated in a Centricon PM 10 tube to 10 mM heme and then reacted with a buffered (pH 9.2) KCN solution (2 M) containing 5 mM sodium dithionite to a final KCN concentration of about 100 mM. Sample preparation and cell assembly were carried out in a nitrogen box.

RESULTS

The resonance Raman spectra were measured at pH 9.2 with 428 and 407 nm laser excitation for the ferrous and ferric cyanide derivatives, respectively. The spectra in the high-frequency region are shown in Figure 1. The π electron density marker line, ν_4, of the ferrous and ferric cyanide derivatives is reported in Figure 1 in comparison with the deoxy and carbonmonoxy HbI derivatives measured under the same experimental conditions. The ν_4 band for ferrous cyanide HbI occurs at 1358 cm^{-1}, at almost the same frequency as for the deoxy derivative. In turn, ferric cyanide HbI peaks at 1373 cm^{-1}, a frequency which is similar to that of carbonmonoxy HbI. Spin and coordination state sensitive lines can also be identified in Figure 1. In particular, ν_3 appears as a single peak at about 1492 and 1506 cm^{-1} for the ferrous cyanide and the ferric cyanide derivatives, respectively; ν_2 is at 1584 cm^{-1} for the ferrous cyanide and at 1578 cm^{-1} for the ferric cyanide adduct. The ν_{10} band cannot be assigned clearly in the ferrous cyanide derivative since it probably overlaps with the vinyl mode at about 1616 cm^{-1}, while it is centered at 1640 cm^{-1} in the ferric adduct.

The iron cyanide stretching bands have been identified in a set of experiments carried out with cyanide isotopes. In Figure 2, the resonance Raman spectra and the associated difference spectra between the $^{12}C^{14}N$ and $^{13}C^{15}N$ adducts of ferrous (A) and ferric (B) HbI are reported. The iron cyanide stretching mode has been detected at 461 cm^{-1} for the ferric derivative and at 455 cm^{-1} for ferrous HbI. No other isotope-sensitive signals were detected in either adduct

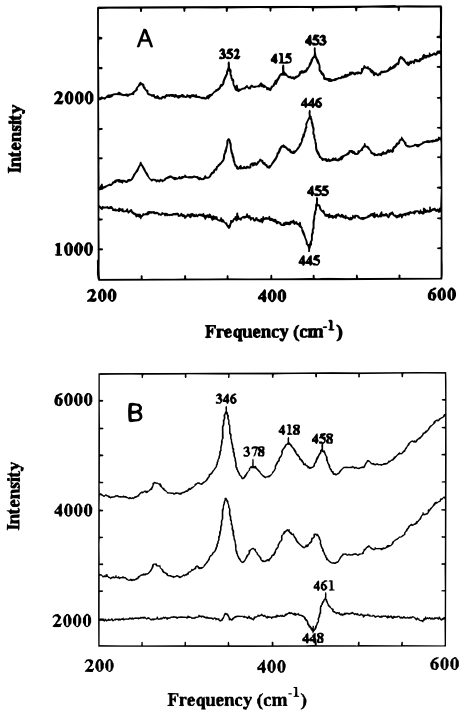

FIGURE 2: Resonance Raman spectra of the $^{12}C^{14}N$ and $^{13}C^{15}N$ isotope adducts of ferrous (A) and ferric HbI (B). Laser excitation wavelength: 428 nm, 10 mW power, in (A); 407 nm, 40 mW power, in (B). From top to bottom: $^{12}C^{14}N$ adduct, $^{13}C^{15}N$ adduct, and difference spectrum ($^{12}C^{14}N$ - $^{13}C^{15}N$).

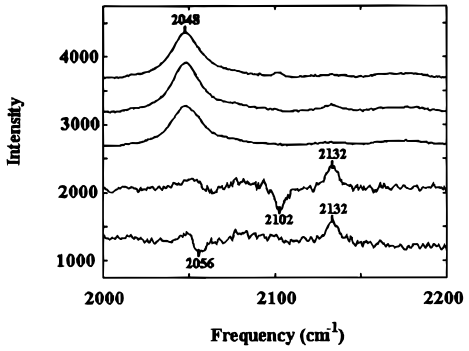

FIGURE 3: Resonance Raman spectra of ferric cyanide HbI. From top to bottom: $^{12}C^{14}N$ adduct, $^{12}C^{15}N$ adduct, $^{13}C^{15}N$ adduct, $^{12}C^{14}N$ minus $^{12}C^{15}N$ difference spectrum, and $^{12}C^{14}N$ minus $^{13}C^{15}N$ difference spectrum. Difference spectra are magnified by a factor of 10. Laser excitation wavelength: 407 nm, 40 mW power.

except for combination bands with the ν_4 peak at 1834 cm^{-1} (461 + 1373 cm^{-1}) for the ferric derivative and at 1813 cm^{-1} (455 + 1358 cm^{-1}) for the ferrous derivative (data not shown). The internal stretching frequency of the bound cyanide in ferric HbI was identified at 2132 cm^{-1} and confirmed by $^{13}C^{15}N$ and $^{12}C^{15}N$ isotopic substitution (Figure 3). The signal originating from the internal stretching mode of the ligand in the ferrous derivative was too weak to be assigned with certainty. Thus FTIR measurements were carried out on concentrated (25 mM) ferrous cyanide protein samples. The FTIR difference spectrum between the $^{12}C^{14}N$ and $^{13}C^{15}N$ adducts of ferrous HbI is shown in Figure 4. The three isotope-sensitive peaks have been assigned to cyanidric acid (2092 cm^{-1}), to the free cyanide ion (2078 cm^{-1}), and to the heme-bound cyanide (2058 cm^{-1}). The frequencies and intensities of the cyanide anion and cyanidric acid are in good agreement with literature values (Yoshikawa et al., 1985). The extinction coefficient for the ferrous cyanide HbI

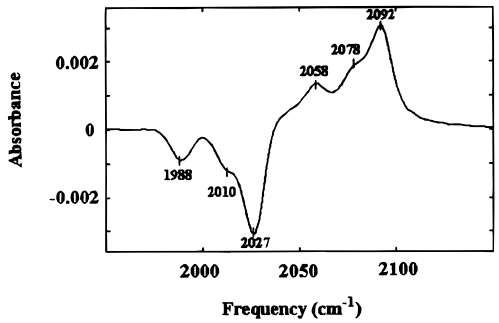

FIGURE 4: FTIR difference spectrum of $^{12}C^{14}N$ minus $^{13}C^{15}N$ ferrous HbI derivatives. The protein concentration was 10 mM in borate buffer, pH 9.2.

adduct is about 0.3 mM^{-1} cm^{-1}, a value in the same range of that reported for horseradish peroxidase (0.42 mM^{-1} cm^{-1}) (Yoshikawa et al., 1985).

DISCUSSION

The resonance Raman spectra in the high-frequency region provide information on the coordination, spin state, and π electron density of heme complexes. In particular, the frequency of the ν_4 band is directly correlated with the π electron density on the macrocycle and hence to the effective overall bond order of the heme. Accordingly, for ferrous ligand-free heme groups (five coordinate high spin) the values of ν_4 fall in the 1355 cm^{-1} region, and for ferric hemes, which are characterized by a lower d_π density, the mode shifts up to the 1370 cm^{-1} range due to depletion of the π^* density in the heme macrocycle and the consequent effective increase in the heme bond order. Coordination to the ferrous heme of ligands that accept π density depletes the heme π^* density to an extent similar to that of the conversion of the iron to the ferric state. Thus, for CO and O_2 derivatives the frequency of ν_4 falls in the 1370−1380 cm^{-1} region.

Other modes in the high-frequency region of the heme resonance Raman spectrum are sensitive to the spin state of the central iron atom. Values of ν_3 and ν_2 in the 1505 and 1580 cm^{-1} regions, respectively, are characteristic of a six-coordinate low-spin configuration for ferric derivatives, and frequencies near 1480 and 1565 cm^{-1}, respectively, are characteristic of six-coordinate high spin. For the ferrous heme ν_3 and ν_2 appear in the 1470 and 1565 cm^{-1} region, respectively, for the five-coordinate high-spin configuration and at 1495 and 1580 cm^{-1}, respectively, for the six-coordinate low-spin configuration. Thus, these lines are reliable markers for the coordination and spin states of the hemes.

In HbI, cyanide binding brings about clear changes to the configuration-sensitive lines of the heme. In the ferric case (Figure 1), the lines at 1506 and 1578 cm^{-1} assigned as ν_3 and ν_2, respectively, confirm the formation of a low-spin adduct. Similarly, as also shown in Figure 1, coordination of cyanide to the ferrous heme shifts ν_3 and ν_2 from 1472 and 1564 cm^{-1} to 1492 and 1582 cm^{-1}, respectively. This confirms that for both oxidation states cyanide coordination results in low-spin adducts.

A surprising feature of cyanide binding to the ferrous heme of HbI is the absence of any significant change in the frequency of ν_4 (1358 cm^{-1}) as compared to its value in the deoxy form (1357 cm^{-1}). This indicates that the π^* electron

density in the heme macrocycle is not depleted from the heme by cyanide coordination in contrast to the behavior observed for the coordination of CO or O_2. The ν_4 frequency for the HbI ferrous cyanide complex is similar to the frequencies reported for ferrous cyanide horseradish peroxidase (Rakshit & Spiro, 1974) and for the bisimidazole iron(II) complex (Choi et al., 1982). The absence of significant π interactions between the cyanide and the heme is further indicated by the C−N stretching frequency in the ferrous complex. Its frequency is located at 2058 cm^{-1}, only 20 cm^{-1} from the free CN^- value (2078 cm^{-1}). A significant extraction of π electron density by the ligand (backbonding) lowers the internal frequency of the ligand as may be seen in the oxy and the carbonmonoxy complexes of heme proteins. We conclude that the bonding of cyanide to the heme of HbI is largely through its σ-bond with little or no evidence for π back-bonding.

The analysis of the low-frequency region of the CN-bound species has brought out several distinctive features concerning the geometry of the Fe−CN grouping. As shown in Figure 2, the direct measurement of the ν(Fe−CN) stretching mode has been reported in parallel for ferrous and ferric HbI. Two major points must be taken into account, namely, the 6 cm^{-1} difference in the ν(Fe−CN) frequency between the ferric and the ferrous HbI derivatives and the absence of other isotope sensitive peaks which could be assigned to bending modes. The small difference in the Fe−CN stretching frequency cleary indicates that the thermodynamic stability of the ferric cyanide derivative with respect to the ferrous one does not depend on the intrinsic Fe−CN bond strength. It may be postulated that the overlap between the d_{z^2} iron orbital and the σ_{2s} cyanide orbital is similar in both derivatives and that the main stabilization factor is given by an electrostatic attraction between the positively charged iron atom and cyanide, which does not contribute directly to the covalency of the bond. On the other hand, inspection of the data in Figures 3 and 4 indicates that the internal stretching frequency of the bound cyanide molecule is very different in the ferrous complex (2058 cm^{-1}) with respect to the ferric derivative (2132 cm^{-1}). This difference has been observed also in the case of ferrous and ferric cyanide derivatives of horseradish peroxidase, microperoxidase, and myoglobin as well as for $Fe^{II}(CN)_6^{4-}$ and $Fe^{III}(CN)_6^{3-}$, suggesting that the same mechanism, namely the interaction of the iron d_π orbitals with the ligand, forms the basis of the frequency decrease in all ferrous compounds. In particular, in comparison to CO and O_2 derivatives there is very little d_π donation from the ferrous iron to the cyanide π^* orbitals. On the other hand, in the ferric complex the higher frequency of the C−N mode with respect to the free ion indicates that the π electron density has moved from the CN^- to the iron porphyrin or in the iron d orbitals.

An additional feature which emerges from inspection of the frequency values is that the cyanide stretching frequencies for ferrous cyanide HbI and horse myoglobin (Reddy et al., 1996) are about 20−30 cm^{-1} higher than that measured under similar conditions in horseradish peroxidase (2029 cm^{-1}) (Yoshikawa et al., 1985) and microperoxidase (2034 cm^{-1}) (Reddy et al., 1996). It is tempting to relate this difference to the different function of these proteins as oxygen carriers or peroxidases. The iron back-donation to the ligand antibonding orbitals, which is responsible for the frequency lowering, must be more efficient in peroxidases in order to favor dissociation of the bound peroxide and formation of the ferryl double-bonded adduct. In contrast, in hemoglobins and myoglobins, the iron d_π orbital donation must be reduced in order to preserve the integrity of the bound ligand. The same general trend is observed for the carbonmonoxide adducts. As reported by Matsukawa (1985), the CO stretching frequencies of peroxidases are always higher than those measured for hemoglobins, and the observed differences between the CO adducts in the two classes of proteins are even more marked than in the case of the cyanide derivatives, due to the larger $d_\pi-\pi^*$ orbital overlap in iron−CO complexes.

In this framework, modulation of function must be accounted for by protein-induced constraints on the extent of the π back-bonding mechanism. Thus, hydrogen bonding, steric forces, and polar interactions may influence the ligand bond order and affect the $d_\pi-\pi^*$ interaction directly (Ray et al., 1994; Li et al., 1994). A hydrogen bond to the bound cyanide ligand provided by the distal histidine has been reported for the crystal structure of ferric legHb (Arutyunyan et al., 1980) and ferric lamprey Hb (Honzatko et al., 1985). However, cyanide is expected to form a stronger H-bond with a protein residue when bound to the ferrous iron, due to the unneutralized negative charge (Yoshikawa et al., 1985). Indeed, protonation of the nitrogen atom to form isocyanic acid brings about a large decrease in the stretching frequency in the free cyanide molecule (ν_{CN^-} = 2078 cm^{-1}, ν_{HCN} = 2092 cm^{-1}, ν_{CNH} = 2058 cm^{-1}) (Botschwina & Sebald, 1983). On this basis, Yoshikawa (1985) proposed that hydrogen bonding occurs between the nitrogen atom of cyanide and the distal histidine in the ferrous horseradish peroxidase adduct and contributes to the observed low-frequency shift. The participation of the distal histidine as a proton donor in the mechanism of cyanide binding to several hemoglobins and myoglobins, including HbI, has been invoked to explain the pH dependence of the rate of cyanide release (Brunori et al., 1992; Boffi et al., 1996).

Nonbonding interactions in the distal pocket must play an important role also in determining the stereochemistry and energetics of the iron cyanide complex. Several mechanisms have been taken into consideration to justify the steric accommodation of bound cyanide in terms of tilted or bent structures. Both structures have been observed in the X-ray crystal structures of ferric hemoglobins and myoglobins adducts. Deathrage (1976) presented evidence that cyanide is bound in a linear fashion, albeit tilted with respect to the heme plane normal, whereas a clearly bent iron cyanide structure has been observed recently in *Aplysia* myoglobin (Conti et al., 1993) and loggerhead sea turtle Hb (Nardini et al., 1995). In *Aplysia* myoglobin, the distal His is absent and cyanide appears to be trapped between a positively charged Arg residue (in position E10) and the iron atom. In loggerhead sea turtle Hb, the distal His is at a distance of 2.75 Å from the cyanide anion and appears to push it off the heme normal.

The tilting mechanism proposed by Deathrage (1976) for sperm whale ferric myoglobin is particularly appealing in that it explains all the observed spectroscopic properties of the HbI−CN adduct. This hypothesis is based on the distortion from planarity of the macrocycle which accompanies the Fe−C−N tilt. As a result, the Fe d_{z^2} orbital is off the heme plane normal, and its rotation is accompanied by the out of plane displacement (ring puckering) in the

opposite direction of the N_1 and N_3 nitrogen atoms. As a consequence the Fe−C−N geometry will be linear, yet tilted with respect to the heme plane normal and the Fe $d_\pi-\pi^*$ orbital overlap unaffected. It is worth noting that a slight distortion of the heme plane due to the N_1 and N_3 pyrrole nitrogen displacement would explain the split of the Q_0 band in the low-temperature visible absorption spectrum of the ferrous cyanide Mb derivative reported recently by Reddy et al. (1996). In fact, the split of the Q_0 electronic transition has been interpreted in terms of removal of the degeneracy of the electronic transition moments along the *x* or *y* directions of the heme plane, an effect which must reflect a structural asymmetry of the macrocycle with a concomitant redistribution of the π orbital electronic charge. It should be pointed out that a distortion of the N_1-N_3 pyrrole nitrogen leaves the iron atom in the "average" heme plane and is fully compatible with its low-spin state. This situation is well adapted to describe the linear geometry of the iron cyanide grouping and the slightly distorted structure of the heme in HbI, given the absence of Raman active bending modes in both the ferrous and ferric adducts. In turn, the split of the Q_0 band is less marked than in horse myoglobin, at 20 °C (Boffi et al., 1996), but is definitely present at 77 K (Boffi, unpublished results).

In conclusion, this study has brought out that cyanide, when it binds to ferrous HbI, has distinct properties from both oxygen and carbon monoxide in that it does not cause major changes in the heme π^* electronic structure. The Raman and FTIR data are consistent with a linear yet tilted Fe−C−N ligand geometry with a concomitant distortion of the heme plane. Comparison with the few resonance Raman and FTIR measurements on ferrous cyanide derivatives in other hemoproteins suggests that the main features of the stereochemistry of this complex must be of general occurrence in the heme-containing oxygen carriers.

In HbI, the stereochemistry of the Fe−CN grouping can be correlated also to the lack of cooperative behavior in cyanide binding (Boffi et al., 1996) whereas the Hill coefficient for oxygen is 1.5. This is additional evidence of the unique mechanism of cooperativity in HbI in which the two hemes communicate with each other through the subunit interface without the major participation of the proximal histidine. In this framework, cyanide would be unable to promote the changes in the heme geometry which are necessary for information transfer. In marked contrast, in HbA cooperativity is observed in the cyanide dissociation reaction as in the case of oxygen (Brunori et al., 1992), indicating that the mechanism of information transfer between hemes must be similar for both ligands. It may be envisaged that in HbA the iron displacement which accompanies ligand binding is sufficient per se to trigger the cooperative mechanism while in HbI iron displacement is decoupled from information transfer.

REFERENCES

Arutyunyan, E. G., Kuranova, I. P., Vainstein, B. K., & Steigenmann, W. (1980) *Krystallografiya 25*, 80−86.

Asher, S. A. (1981) *Methods Enzymol. 76*, 371−413.

Boffi, A., Takahashi, S., Spagnuolo, C., Rousseau, D. L., & Chiancone, E. (1994) *J. Biol. Chem. 269*, 20437−20440.

Boffi, A., Ilari, A., Spagnuolo, C., & Chiancone, E. (1996) *Biochemistry 35*, 8068−8074.

Botschwina, P., & Sebald, P. (1983) *J. Mol. Spectrosc. 100*, 1−23.

Brancaccio, A., Cutruzzolà, F., Travaglini Allocatelli, C., Brunori, M., Smerdon, S. J., Wilkinson, A. J., Dou, Y., Keenan, D., Ikeda-Saito, M., Brantley, R. E., & Olson, J. (1994) *J. Biol. Chem. 269*, 13843−13853.

Brunori, M., Antonini, G., Castagnola, M., & Bellelli, A. (1992) *J. Biol. Chem. 267*, 2258−2263.

Chiancone, E., Vecchini, P., Verzili, D., Ascoli, F., & Antonini, E. (1983) *J. Mol. Biol. 152*, 577−592.

Ching, Y. C., Argade, P. V., & Rousseau, D. L. (1985) *Biochemistry 24*, 4938−4946.

Choi, S., Spiro, T. G., Langry, K. C., Smith, K. M., Budd, D. L., & La Mar, G. N. (1982) *J. Am. Chem. Soc. 104*, 4345−4351.

Conti, E., Moser, C., Rizzi, M., Matttevi, A., Lionetti, C., Coda, A., Ascenzi, P., Brunori, M., & Bolognesi, M. (1993) *J. Mol. Biol. 233*, 498−508.

Deathrage, J. F., Loe, S. L., Anderson, C. M., & Moffat, K. (1976) *J. Mol. Biol. 104*, 687−706.

Honzatko, R. B., Hendrickson, W. A., & Love, W. E. (1985) *J. Mol. Biol. 184*, 147−164.

Ilari, A., Boffi, A., & Chiancone, E. (1995) *Arch. Biochem. Biophys. 316*, 378−384.

Keilin, D., & Hartree, E. F. (1955) *Biochem. J. 61*, 153−171.

Matsukawa, S., Mawatari, K., Yoneyama, Y., & Kitagawa, T. (1985) *J. Am. Chem. Soc. 105*, 1108−1112.

Nardini, M., Tarricone, C., Rizzi, M., Lania, A., Desideri, A., De Sanctis, G., Coletta, M., Petruzzelli, R., Ascenzi, P., Coda, A., & Bolognesi, M. (1995) *J. Mol. Biol. 247*, 459−465.

Peng, S. M., & Ibers, J. A. (1976) *J. Am. Chem. Soc. 96*, 5295−5296.

Rakshit, G., & Spiro, T. (1974) *Biochemistry 13*, 5317−5323.

Ray, G. B., Li, X.-Y., Ibers, J., Sessler, J., & Spiro, T. G. (1994) *J. Am. Chem. Soc. 116*, 162−176.

Reddy, K. S., Yonetani, T., Tsuneshige, A., Chance, B., Kushkuley B., Stavrov, S. S., & Vanderkooi, J. M. (1996) *Biochemistry 35*, 5562−5570.

Scheidt, W. R., Lee, Y. J., Luangdilok, W., Haller, K. J., Anzai, K., & Hatano, K. (1983) *Inorg. Chem. 22*, 1516−1525.

Song, S., Boffi, A., Chiancone, E., & Rousseau, D. L. (1993) *Biochemistry 32*, 6330−6336.

Yoshikawa, S., O'Keeffe, D. H., & Caughey, W. S. (1985) *J. Biol. Chem. 260*, 3518−3528.

Yu, N. T. (1986) *Methods Enzymol. 130*, 350−415.

Yu, N. T., Benko, B., Kerr, E. A., & Gersonde K. (1984) *Proc. Natl. Acad. Sci. U.S.A. 81*, 5106−5110.

BI9618880